A strategy of fabricating exfoliated thermoplastic polyurethane/clay nanocomposites via introducing maleated polypropylene

Xiaoyu Meng [a,b], Zhe Wang [a,b], Haiou Yu [a,b], Xiaohua Du [a,b], Shiyun Li [a,b], Yanhui Wang [a], Zhiwei Jiang [a], Qiaoyi Wang [c], Tao Tang [a,*]

[a] State Key Laboratory of Polymer Physics and Chemistry, Changchun Institute of Applied Chemistry, Chinese Academy of Sciences, Changchun 130022, China
[b] Graduate School of the Chinese Academy of Sciences, Beijing 100039, China
[c] College of Chemistry, Jilin University, Changchun 130012, China

ABSTRACT

By reducing the attraction between the platelets of octadecylammonium chloride modified montmorillonite (OMMT-C18) via pre-intercalation of maleated polypropylene (MAPP), OMMT-C18 was exfoliated in thermoplastic polyurethane (TPU) matrix during melt-mixing. Wide angle X-ray diffraction, transmission electron microscopy and thermogravimetric analysis were used to investigate the microstructure of TPU nanocomposites. Three factors (including introducing sequence, the kind and the content of MAPP) showed important effects on the dispersion degree of OMMT-C18 in TPU matrix. The results confirmed that the pre-intercalation of MAPP was necessary for the exfoliation of OMMT-C18; however, the role of MAPP in TPU nanocomposites was different from that in polypropylene nanocomposites. In addition, the investigation on the morphology evolution of TPU nanocomposites showed that shear force played a key role in the formation of exfoliated TPU nanocomposites. TPU nanocomposites with exfoliated structure showed better properties compared with TPU and its nanocomposites with intercalated structure.

© 2009 Elsevier Ltd. All rights reserved.

1. Introduction

For many of desired benefits of adding fillers to polymers, improvements are achieved when organically modified montmorillonites (OMMT) are homogeneously exfoliated in polymer matrices [1–8]. Fig. 1 presents two possible routes to exfoliate OMMT in a polymer matrix during melt-mixing [9,10]. Generally, the exfoliation of OMMT takes place when the attraction (labeled f_1) between OMMT sheets, such as van der Waals force and electrostatic interaction, is broken via molecular diffusion or shear process. The interaction (labeled f_2) between polymer and OMMT and the melt viscosity (labeled η_m) of polymer matrix are two important factors. The former is related to the chemical structures of polymers and the modifiers, and the modifier content in the OMMT.

Balazs et al. proposed the certain types of polymers facilitating the penetration into the gallery of OMMT [9]. These polymers contain a fragment highly attracted to OMMT sheets and a longer fragment not attracted to the MMT sheets, which attempt to gain entropy by pushing the sheets apart. In this case, the exfoliated structure can be created via the diffusion of polymer (Fig. 1a).

Otherwise the mixture will be immiscible or forms an intercalated structure. For instance, polypropylene (PP) has no fragment attracted to OMMT layers, consequently the mixture of PP and OMMT is immiscible; whereas polyamide-12 has stronger attraction with OMMT layers but shorter hydrophobic fragment, and thus only intercalated structure is created via the molecular diffusion [10]. In the latter case, the intercalated structure results from the binding of the polymer between two surfaces [9,11]. However, the exfoliated structure is created when f_1 is broken by a shear force [10]. Stronger f_2 between OMMT and polymers and higher η_m favor the exfoliation of clay sheets (Fig. 1b). In some case, the interaction between alkylammonium ion modified OMMT and polar polymers is weaker, and the fragment not attracted to the layers is shorter, such as thermoplastic polyurethane (TPU). Therefore, it is difficult that OMMT modified by alkylammonium ion is directly exfoliated in TPU matrix via molecular diffusion or even shear process [12,13].

A conventional strategy for the exfoliation of OMMT in TPU matrix is to increase the f_2 for promoting the transfer of shear stress. In the previous reports, OMMT modified with alkyl tallow quaternary ammonium ion could not be exfoliated in TPU matrix, whereas OMMT modified by the surfactant containing hydroxyl group (such as Cloisite 30B (30B)) was exfoliated in TPU matrix by melt-mixing [12–14], attributed to the stronger f_2 between 30B and TPU [15]. Another feasible strategy is to decrease the f_1 for reducing
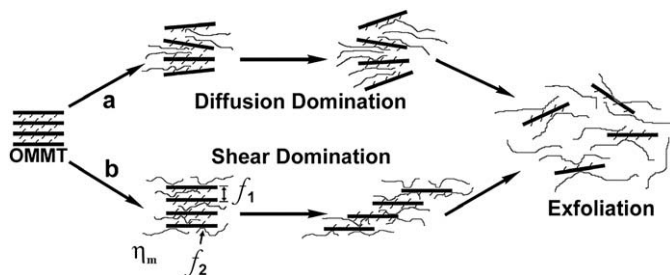
Fig. 1. The scheme of exfoliation process of OMMT. f_1: the attraction between OMMT sheets; f_2: the interaction between OMMT and polymer; η_m: the melt viscosity of polymer matrix.

the resistance of the exfoliation of platelets under shear stress. Previous researches have showed that the f_1 weakened as the interlayer distance increased [16,17]. The expansion of interlayer distance is habitually obtained by the modification of quaternary ammonium salts, and the increase of content and tallow number of the surfactant benefits the expansion of gallery [18,19]. However, the alkyl chains of surfactant weaken the f_2 and then decrease the transfer of shear stress [19], thus the f_2 is not large enough to overcome the f_1 by simply increasing the contents of alkylammonium ions in the OMMT.

In this work, we demonstrated a novel methodology for the exfoliation of OMMT modified by alkylammonium ion in TPU matrix via reducing the f_1 by introducing a functionalized polymer into the interlayer of OMMT. Introducing maleated polypropylene (MAPP) was an appropriate choice to accomplish a larger interlayer distance because the molecular structure of MAPP contains anhydride group highly attracted to OMMT sheets and a longer nonpolar fragment not attracted to the MMT sheets. Moreover, there are some compatibility between MAPP and TPU due to strong interactions, such as hydrogen bonding [20] and chemical reaction [21], which can transfer the shear stress provided by TPU matrix to OMMT. In addition, blending two or more polymer is a technique for balancing properties [22,23]. In the case of TPU, the addition of polyolefin in TPU can reduce the cost and improve thermal stability, mechanical properties (e.g., modulus, strength), and processing performance of TPU [20,24,25]. Thus the introducing MAPP might promote not only the dispersion of OMMT but also the properties of TPU matrix. A recent report has showed that adding MAPP could improve not only the dispersion of OMMT (such as Cloisite 25A and 30B) in TPU matrix during melt-mixing but also the mechanical properties of the resultant TPU nanocomposites [26]. Unfortunately, the effects of introducing sequence of MAPP, the kind and the content of MAPP on the dispersion degree of OMMT in TPU matrix were not studied. According to the results of transmission electron microscope (TEM) and wide angle X-ray diffraction (WAXD) in this work, the above three factors showed important effects on the dispersion degree of OMMT-C18 in TPU matrix. Moreover, based on the chemical and physical effects of OMMT-C18 on the polymers, thermogravimetric analysis (TGA) was developed to characterize the microstructure of ternary composites, which provided more detailed information of morphology.

2. Experimental section

2.1. Materials

Na$^+$-montmorillonite (MMT, with a cation exchange capacity (CEC) of 119 meq/100 g) used in this work was from Kunimine Co. Octadecylamine was from Wako Pure Chemical Industries Co. Thermoplastic polyurethane (TPU, $M_w = 177\,000$) was purchased

from Urethane Company at Yantai. The TPU consists of a 1000 g/mol poly(tetramethylene oxide) (PTMO) soft segment with a 4,4′-methylene diphenyl diisocyanate (MDI) and 1,4-butanediol (BDO) hard segment. The hard segment concentration is 55 wt%, and the shore hardness is 85A. Two maleated polypropylenes (MAPP) with 4.6 and 2.3 wt% of MA group were supplied by Sanyo Co., and labeled as MAPP-1010 ($M_w = 30\,000$) and MAPP-1001 ($M_w = 40\,000$), respectively. All the materials were dried in a vacuum oven at 80 °C for 12 h before using.

2.2. Sample preparation

Modified MMT by octadecylammonium chloride (OMMT-C18) was synthesized as described in our previous papers [18,27]. The octadecylammonium chloride loading with 100% CEC was added in the process of modification, and the surfactant adsorption level was 65.4% CEC according to the thermogravimetric analysis. The pre-mixtures of MAPPs and OMMT-C18 were prepared at 185 °C in a Brabender with a rotating speed of 100 rpm for 15 min. The resultant pre-mixtures with different composition by weight were labeled as P-1 (MAPP-1010/OMMT-C18 = 2/1), P-2 (MAPP-1001/OMMT-C18 = 2/1), P-3 (MAPP-1010/OMMT-C18 = 1/1) and P-4 (MAPP-1001/OMMT-C18 = 4/1), respectively. OMMT-C18 or the pre-mixtures were melt-mixed with TPU at 185 °C in a Brabender with a rotating speed of 100 rpm for 10 min. The neat TPU underwent the same process with the blend samples. In order to investigate the effect of MAPP, TPU composites were prepared via different mixing sequences. Composite-1: OMMT-C18 mixed with TPU; Composite-2: OMMT-C18 premixed with MAPP-1010 and then mixed with TPU; Composite-3: OMMT-C18, MAPP-1010 and TPU mixed simultaneously; Composite-4: OMMT-C18 premixed with TPU firstly and MAPP-1010 was introduced; Composite-5: MAPP-1010 premixed with TPU and the blend was compounded with OMMT-C18. All TPU composites contained 5 wt% of OMMT-C18 and 10 wt% of MAPP.

2.3. Characterization

Wide angle X-ray diffraction (WAXD) was carried out with a Rigaku model D max 2500 with a Cu Kα radiation. The morphologies of the composites were observed by transmission electron microscope (TEM, JEOL2010) on microtome sections of the composites. Ultrathin sections were cryogenically cut at a temperature of −80 °C using a Leica Ultracut. The ultrathin sections of TPU composites were slightly stained by RuO$_4$ vapor at 30 °C for 3 h to enhance the phase contrast. Fourier transform infrared spectroscopy (FTIR) was performed on BRUKER Vertex 70 at a resolution of 2 cm^{-1}. Thermogravimetric analysis (TGA) was carried out with SDT Q600 under N$_2$ with a heating rate of 10 °C/min, and the TPU composites were extracted by tetrahydrofuran (THF) in a Soxhlet apparatus for 48 h to get rid of TPU chains not tethering on OMMT layers. Static mechanical properties were measured with Instron 1121 tensile testing machine, and the crosshead rate was set at 20 mm/min, the testing bars were prepared by compression molding. For each data point, five samples were tested and the average value was taken. The oxygen transmission rate was measured with a G.T.R. measurement apparatus K-315-N-03 at 30 °C, and the thickness of sample was about 30 μm. All the samples were dried in a vacuum oven at 80 °C for 12 h before characterization.

3. Results and discussion

The results of WAXD prove that the OMMT modified by octadecylammonium chloride (OMMT-C18) cannot be directly exfoliated in TPU matrix (Fig. 2). Although the chains of TPU quickly
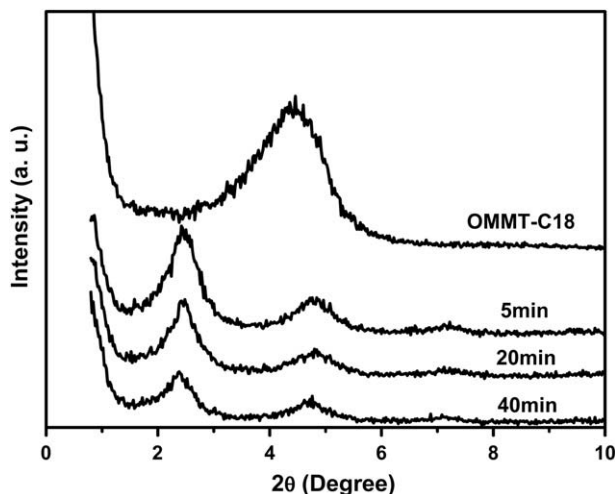
Fig. 2. WAXD profiles of TPU/OMMT-C18 nanocomposites mixed for different times.

intercalate into the interlayers of OMMT-C18, the interlayer distance remains unchanged as the mixing time increases. Ultimately only intercalated structure is obtained when processed for 40 min. It confirms that the TPU cannot break the f_1 between OMMT-C18 sheets to exfoliate the platelets.

3.1. The effect of introducing sequence of maleated polypropylene (MAPP)

In order to reduce the f_1 of OMMT-C18 and finally realize the exfoliation of the OMMT-C18 in TPU matrix, a kind of MAPP with 4.6 wt% MA (MAPP-1010) is introduced to promote the formation of exfoliated TPU nanocomposite. Four introducing sequences of MAPP (see Experimental section) are applied to adjust the f_1 between the platelets and the η_m of polymer matrix, which are profitable to gain insight into the effects of these parameters on the microstructure of TPU nanocomposites.

3.1.1. Investigation on microstructure of the composites by means of WAXD and TEM

The WAXD profiles and the morphologies of the composites compounded by different sequences are compared in Fig. 3. The

weight ratio of OMMT-C18 and MAPP-1010 is 1:2. When MAPP-1010 is not introduced into the system (Composite-1), only intercalated structure is obtained, and many larger aggregates exist in the matrix (Fig. 3b). When OMMT-C18 is pre-mixed with MAPP-1010 (the pre-mixture is labeled as P-1), the best dispersion is achieved (Composite-2). The (001) diffraction peak of OMMT-C18 disappears in WAXD profile and the MMT platelets are exfoliated homogenously (Fig. 3c). In this case, the chains of MAPP-1010 in P-1 can sufficiently intercalate into the galleries and the larger interlayer distance is achieved, accordingly the f_1 is lower. Therefore the shear stress transferred from TPU matrix can overcome the f_1 easily. The samples for TEM observation are also slightly stained by RuO_4 to discern different polymer phases (Fig. 4). In these TEM images, besides MMT phase, MAPP-1010 phase (bright island-like region) can be further distinguished from TPU phase (dark sea-like region). Fig. 4a suggests that many exfoliated platelets in Composite-2 contact with both TPU phase and MAPP-1010 phase at the same time. The high-magnification image distinctly shows that one side of the sheet is located in MAPP-1010 phase and the other side in TPU phase (Inset in Fig. 4a). Clearly, owing to the favorable interaction between OMMT-C18 and MAPP-1010 [28], the platelets still contact with MAPP-1010 phase when the exfoliation is achieved.

When OMMT-C18, MAPP-1010 and TPU are mixed simultaneously (Composite-3), a weaker broad diffraction peak appears in the WAXD profile. In the TEM image, exfoliated and intercalated states coexist in the matrix (Fig. 3d). Both MAPP-1010 and TPU have favorable interaction with OMMT-C18 and can intercalate into the interlayers quickly, thereby many OMMT-C18 platelets exist at the interface between MAPP-1010 phase and TPU phase (Fig. 4b). Owing to lower content of MAPP-1010 in the system, however, the intercalation probability of MAPP-1010 should be lower than that of TPU. Meanwhile the strong interaction between MAPP and TPU makes further intercalation of some MAPP-1010 chains difficult. Therefore the intercalated levels of OMMT-C18 are discrepant, and different interlayer distances appear in the composite. Some particles with larger interlayer distance are exfoliated, whereas the particles with smaller interlayer distances still exist as intercalated states.

When OMMT-C18 is pre-mixed with TPU and then MAPP-1010 is introduced (Composite-4), a stronger broad diffraction peak appears (Fig. 3e). As the interlayer distance of OMMT-C18 does not change after some TPU chains intercalate into the galleries in TPU matrix (Fig. 2), the broad peak should mainly stem from the
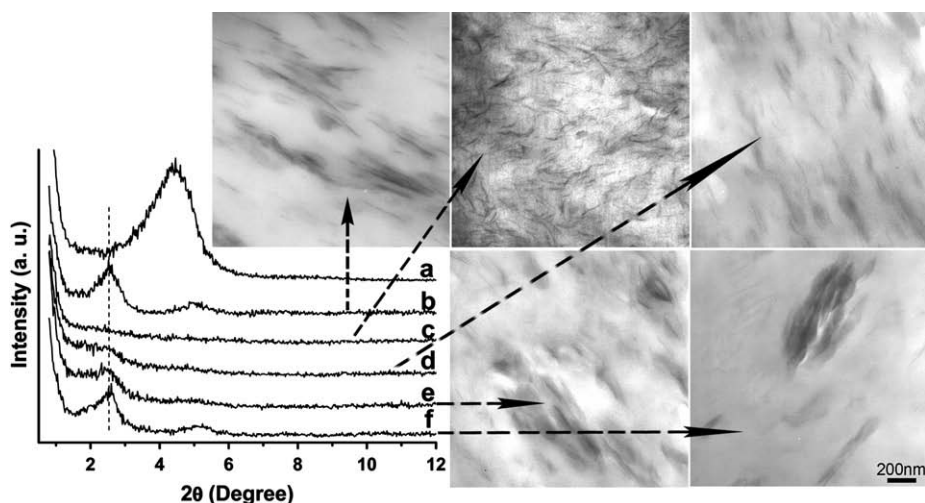

Fig. 3. WAXD profiles and TEM images of TPU nanocomposites prepared by different mixing sequences. (a) OMMT-C18; (b) Composite-1; (c) Composite-2; (d) Composite-3; (e) Composite-4; (f) Composite-5.
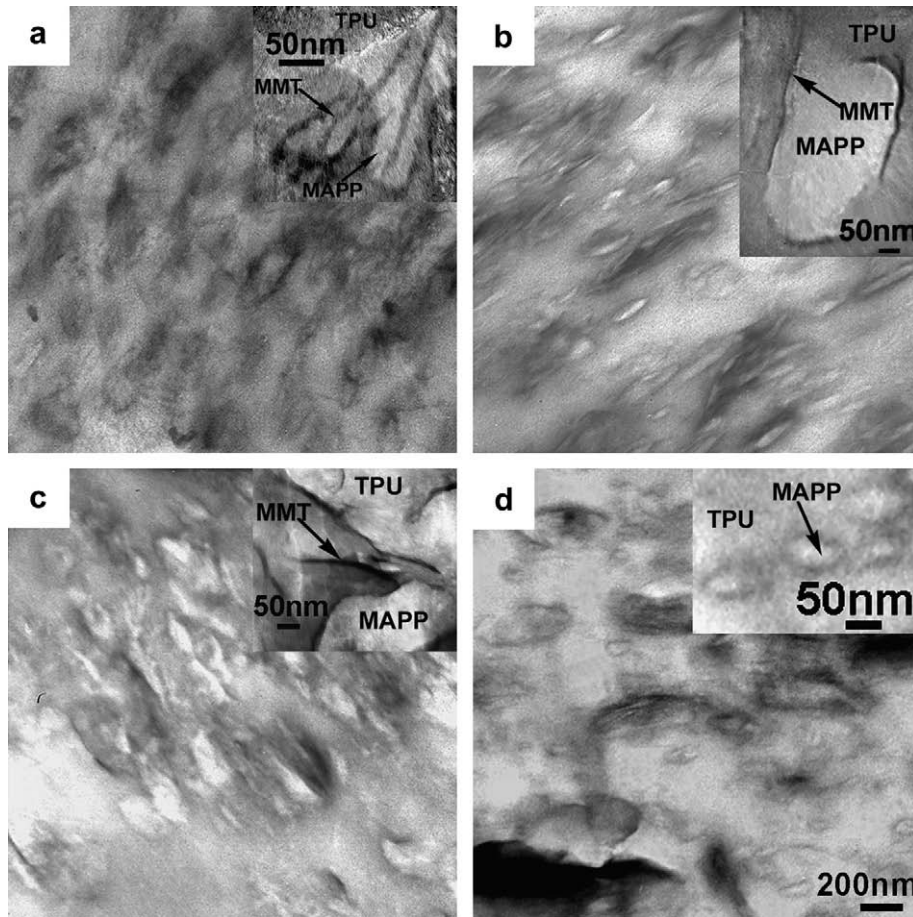
Fig. 4. TEM images of TPU composites stained by RuO$_4$. (a) Composite-2; (b) Composite-3; (c) Composite-4; (d) Composite-5.

intercalation of MAPP-1010. MAPP-1010 with a lower molecular weight can interact with the surface of OMMT-C18 and even react with the surfactant of OMMT-C18 [28]. Although TPU is not miscible with MAPP-1010 at molecular level, there is still the compatibility between TPU and MAPP-1010 resulting from the presence of the strong interaction. Thus some chains of MAPP-1010 can intercalate into the galleries occupied by TPU chains. A similar phenomenon has been reported in poly(ethylene oxide)/poly-(methyl methacrylate)/OMMT system [29]. The following results of thermogravimetric analysis (TGA) also prove the intercalation of MAPP-1010 in this case. However the amount of MAPP-1010 intercalating into the interlayers is smaller. TEM image shows that most of OMMT-C18 platelets exist in TPU phase and some OMMT-C18 platelets exist at the interface between TPU phase and MAPP-1010 phase (Fig. 4c). A small amount of intercalated MAPP has no contribution to the exfoliation as the achievement of larger distance is difficult in this case.

When MAPP-1010 and TPU are pre-mixed (Composite-5), the interlayer distance of OMMT-C18 is the same as that of Composite-1. But the particles are very inhomogeneous, and some particles are even larger than those in OMMT-C18/TPU system (Fig. 3). Most of MA groups in the MAPP form hydrogen bond and/or even react with the functional groups (such as NH) in the chains of TPU after pre-mixing with TPU for a longer time at high temperature [20,21]. As a result, few of anhydride groups in MAPP-1010 can interact with OMMT-C18. In this case, almost no MAPP-1010 intercalates into the galleries of OMMT-C18 that is dispersed in TPU matrix. The high-magnification TEM images show no OMMT-C18 platelets in MAPP-1010 phase (Fig. 4d). Thus only TPU chains intercalate into the

galleries, and the interlayer distance is the same as that of Composite-1. In addition, because the η_m of MAPP-1010/TPU blend is lower than that of neat TPU (Fig. 5), the shear stress provided by the matrix will weaken [30]. In this case, all MAPP-1010 molecules reside in the TPU phase, thus the η_m is the lowest among these composites. The smallest interlayer distance and the weakest shear stress provided by the matrix result in the poor dispersion of OMMT-C18 in TPU matrix.
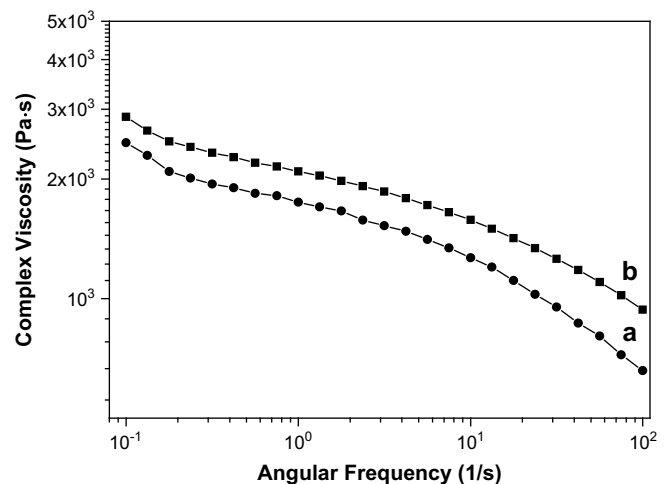

Fig. 5. Complex viscosity of (a) the blend of MAPP-1010/TPU = 10/85 (by weight) mixed at 185 °C for 10 min; (b) neat TPU processed under the same conditions.
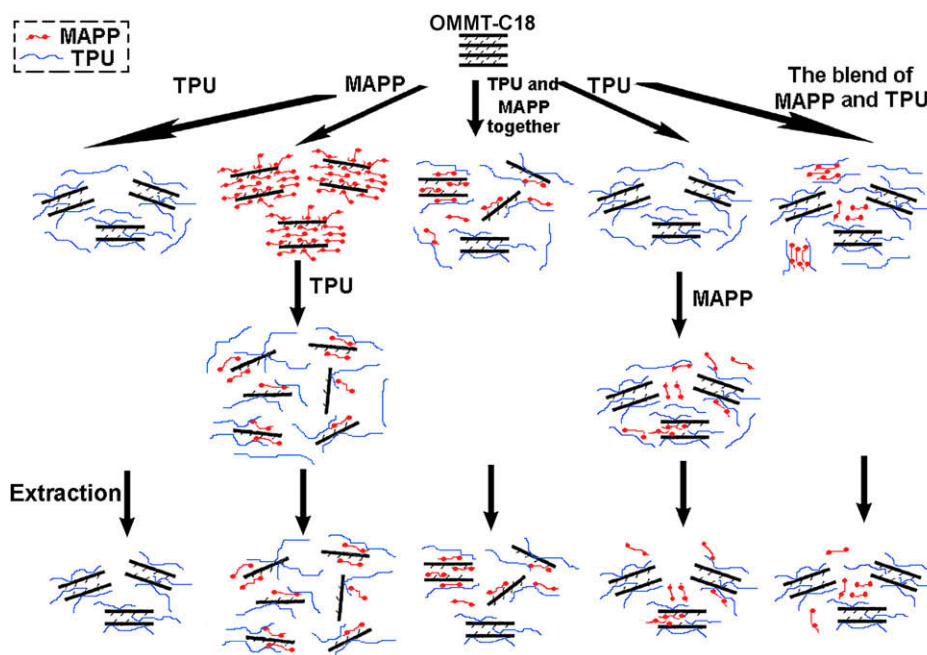
Fig. 6. Scheme of morphology evolution of TPU composites prepared with different mixing sequences.

Based on the above results, the microstructural schemes of TPU composites prepared by different compounding sequences are summarized in Fig. 6. When MAPP-1010 is not introduced into the system, only intercalated structure is obtained. When OMMT-C18 is pre-mixed with MAPP-1010, the best dispersion is achieved. When OMMT-C18, MAPP-1010 and TPU are mixed simultaneously, exfoliated and intercalated states coexist in the matrix. When OMMT-C18 is pre-mixed with TPU and then MAPP-1010 is introduced, a small amount of intercalated MAPP has no contribution to the exfoliation as the achievement of larger distance is difficult in this case. When MAPP-1010 and TPU are pre-mixed, only TPU chains intercalate into the galleries and the dispersion of OMMT-C18 is poor.

3.1.2. Investigation on microstructure of the composites by means of TGA

TGA is employed to further confirm these microstructures. Generally OMMT has two effects on the thermal degradation of polymers, i.e. physical barrier effect and chemical effect. The MMT platelets can delay the volatilization of degradation products of polymers, and thereby the temperature of weight loss will rise [31,32]. However, the acidic sites on the OMMT, formed by decomposition of the surfactants, can accelerate the degradation of polymer [33–35], and the temperature of weight loss will reduce. Comparing with the physical barrier effect, the chemical effect of OMMT on the degradation of polymer mainly depends on the direct contact between two components. Therefore the variety of morphology in the composites will result in the different behaviors of weight loss.

In the differential thermogravimetric (DTG) plots (Fig. 7), the neat TPU (curve A in Fig. 7a) shows two maximum temperatures of weight loss (T_{max}), and the one at lower temperature is caused by the degradation of hard segment, and the soft segment is responsible for the other one [36]. When TPU is mixed with MAPP-1010, the degradation peak of hard segment splits into two peaks, and T_{max} of the soft segment remains unchanged (curve D in Fig. 7a). It suggests that MAPP accelerates the degradation of hard segment due to possible chemical reaction of NH group with anhydride group of MAPP [21], and accordingly T_{max} of the hard segment interacting
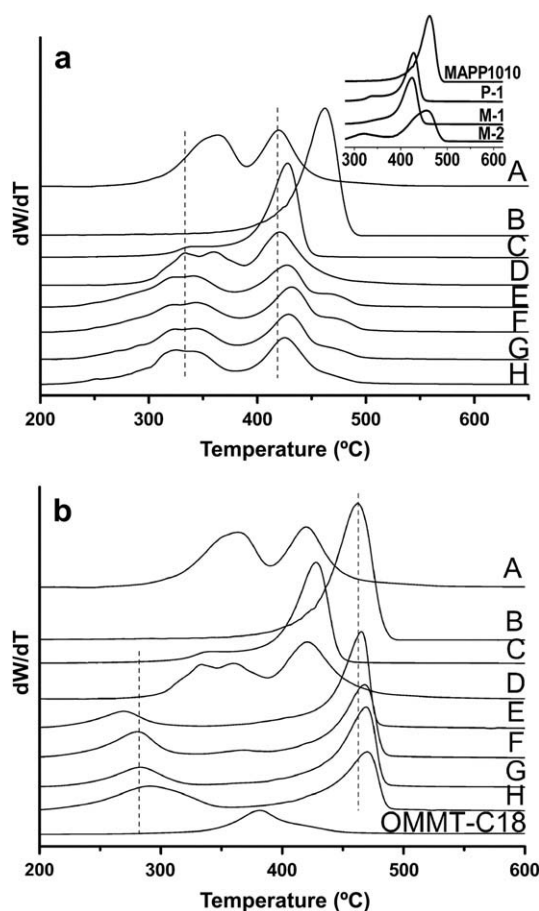

Fig. 7. Differential thermogravimetric (DTG) plots. Curves: A. TPU; B. MAPP-1010; C. P-1; D. MAPP-1010/TPU blend; E. Composite-2; F. Composite-3; G. Composite-4; H. Composite-5. E, F, G, H in (a) are the samples before extraction with THF; E, F, G, H, in (b) are the samples after extraction with THF. Insets in (a), M-1: MAPP-1010/OMMT-C18 = 1/1 physical mixture at room temperature (by weight); M-2: (TPU/OMMT-C18 composite)/MAPP-1010 = (40/10)/50 physical mixture at room temperature (by weight).

with MAPP-1010 decreases, whereas MAPP-1010 has no effect on the soft segment. In the TPU composites (curves E–H in Fig. 7a), the T_{max} of hard segment further decreases comparing with that of MAPP/TPU blend, whereas the T_{max} of soft segment increases. Owing to the stronger interaction between OMMT and the hard segment, the most OMMT platelets contact with the hard segment of TPU, thus the acidic sites of OMMT-C18 accelerate the degradation of hard segment. However the chemical effect of OMMT has no effect on the soft segment, and the physical barrier of MMT platelets plays a dominating role during the degradation of soft segment, so the T_{max} of soft segment increases. T_{max} of MAPP-1010 in P-1 decreases comparing with neat MAPP-1010 (curve B vs. C in Fig. 7a), suggesting that the chemical effect of OMMT-C18 plays a dominating role in the system. Even if OMMT-C18 is not pre-intercalated by MAPP-1010 chains, OMMT-C18 also accelerates thermal degradation of MAPP-1010, which is proved by DTG plot of the physical mixture of MAPP-1010 and OMMT-C18 with the same composition as P-1 (M-1) prepared at room temperature (the inset of Fig. 7a). The T_{max} of MAPP-1010 in M-1 shifts to lower temperature, similar to that of P-1. However, the degradation of MAPP is not influenced when OMMT-C18 is surrounded by TPU chains. In the DTG plot of the mixture of TPU/OMMT-C18 composite and MAPP-1010 at room temperature (M-2), a broad peak appears ranging from 400 to 500 °C, which results from the weight loss of both the soft segment of TPU and MAPP-1010. The physical barrier of MMT platelets results in the increase of T_{max} of the soft segment comparing with neat TPU. Owing to the surrounding of TPU chains, the acidic sites on the OMMT-C18 have no influence on MAPP-1010, thus the T_{max} of MAPP-1010 in M-2 is the same as that of neat MAPP-1010.

Owing to the lower content of MAPP, the peaks of MAPP-1010 in the DTG plots of TPU composites are weak (curves E–H in Fig. 7a), thereby these composites were extracted by tetrahydrofuran (THF) to get rid of TPU chains not tethering on OMMT-C18 platelets, and the morphological scheme after extraction is also shown in Fig. 6. In the DTG plots (Fig. 7b), the peaks of TPU chains in the range from 310 °C to 450 °C disappear, and the peak of MAPP-1010 is shown distinctly. The T_{max} of MAPP-1010 in the extracted TPU composites increases for different levels comparing with neat MAPP-1010. The difference of T_{max} should be ascribed to the discrepant physical barrier and chemical effect of MMT platelets in these composites. Although the best dispersion of OMMT-C18 can result in the obvious physical barrier effect in Composite-2, unfortunately the chemical effect of OMMT-C18 on the degradation of MAPP is also the strongest in this case since many OMMT-C18 platelets still contact with MAPP-1010 when the exfoliation is achieved (Fig. 4a). Ultimately the increase of T_{max} is the smallest in all the composites. In Composite-3 and Composite-4, less MAPP-1010 contact with OMMT-C18 platelets, and the chemical effect of OMMT-C18 is weaker, consequently the T_{max} of MAPP-1010 is higher comparing with that in Composite-2. In Composite-5, almost no MAPP-1010 can contact with OMMT-C18, thus OMMT-C18 has only physical barrier effect on MAPP-1010. Therefore the T_{max} of MAPP-1010 has an obvious increase in spite of the poor dispersion of OMMT in this case.

The degradations ranging from about 270–290 °C in curves E–H of Fig. 7b should result from the TPU chains tethering on the surface of OMMT-C18 (The T_{max} of OMMT-C18 is about 380 °C). Owing to high weight ratio of OMMT-C18 to TPU in the extracted composites, both the hard segment and the soft segment of TPU tethering on OMMT-C18 platelets are influenced by the acidic sites of OMMT-C18. Thus the peaks of hard segment and soft segment combine to one peak, which has been further proved by the degradation of TPU/OMMT-C18 = 1/4 (by weight) composite. Owing to higher content of OMMT-C18 in TPU/OMMT-C18 = 1/4 composite, most of TPU chains intercalate into the galleries of OMMT-C18. In this case, the degradation processes of both the hard segment and the soft segment can

be strongly influenced by OMMT-C18, thus TPU has only one peak of weight loss. In Composite-2, the OMMT-C18 platelets are exfoliated and the contact area between OMMT-C18 and TPU is the largest, thus the chemical effect of OMMT-C18 is the most remarkable, and the T_{max} of TPU is the lowest in this composite. In contrast, the dispersion state of OMMT-C18 in Composite-5 is the poorest among all TPU composites, and the contact area between OMMT-C18 and TPU is the smallest. Therefore the chemical effect of OMMT-C18 is the weakest, and the T_{max} of TPU is the highest in this composite. TGA results are consistent with those of WAXD and TEM, which further discern the morphologies of TPU composites.

3.2. The effects of the kind and the content of MAPP

The above results suggest that the pre-intercalation of MAPP is necessary to the formation of exfoliated OMMT-C18 in TPU matrix. However, the pre-intercalation of MAPP will be influenced by grafting degree of MA group, η_m (melt viscosity) and the content of MAPP. The interaction between MAPP and OMMT-C18 is the thermodynamic driving force for the intercalation of PPMA. The lower η_m will provide a favorable environment for molecular diffusion. The variation of these factors will result in the difference of f_1 and f_2 shown in Fig. 1, which will influence the dispersion state of OMMT-C18. As a control, MAPP with 2.3 wt% MA (MAPP-1001) was also used to prepare a pre-mixture of MAPP-1001/OMMT-C18 = 2/1 (by weight) (P-2). The molecular weight of MAPP-1001 is higher than that of MAPP-1010, meaning that the molecular diffusion of MAPP-1001 is more difficult comparing with MAPP-1010 due to higher η_m (Fig. 8). More importantly, the higher MA content in MAPP-1010 promotes the intercalation of MAPP-1010 into the galleries of OMMT-C18 due to the stronger interaction between MAPP-1010 and OMMT-C18. Therefore the larger interlayer distance is achieved in P-1 comparing with P-2, and the f_1 is smaller in the P-1. WAXD results show that the (001) diffraction peak of OMMT-C18 disappears after mixing P-1 with TPU for 10 min, but the position of the (001) diffraction peak for OMMT-C18 remains unchanged after mixing P-2 with TPU under the same mixing conditions (Fig. 9a and b). Meanwhile TEM images show that the OMMT-C18 platelets are exfoliated homogeneously in TPU/P-1 composite, whereas many intercalated structure still exist in TPU/P-2 composite (Fig. 9a and b). It can be ascribed to the following reasons. On one hand, OMMT-C18 could be exfoliated easily in TPU/P-1 composite due to smaller f_1. On the other hand, more MA groups of MAPP-1010 strengthen the f_2 due to hydrogen bonding and/or even chemical reaction between
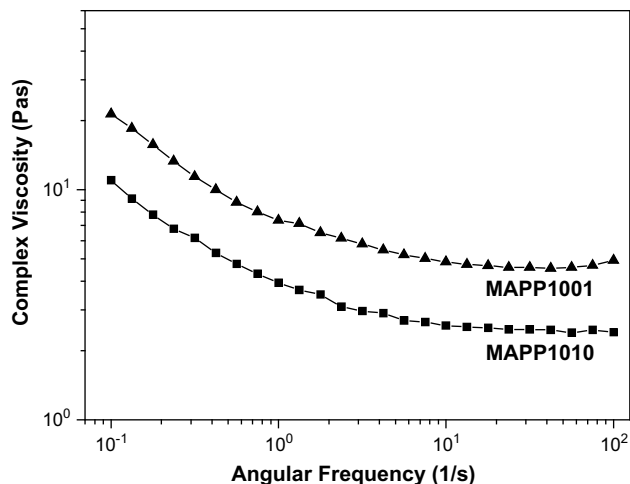

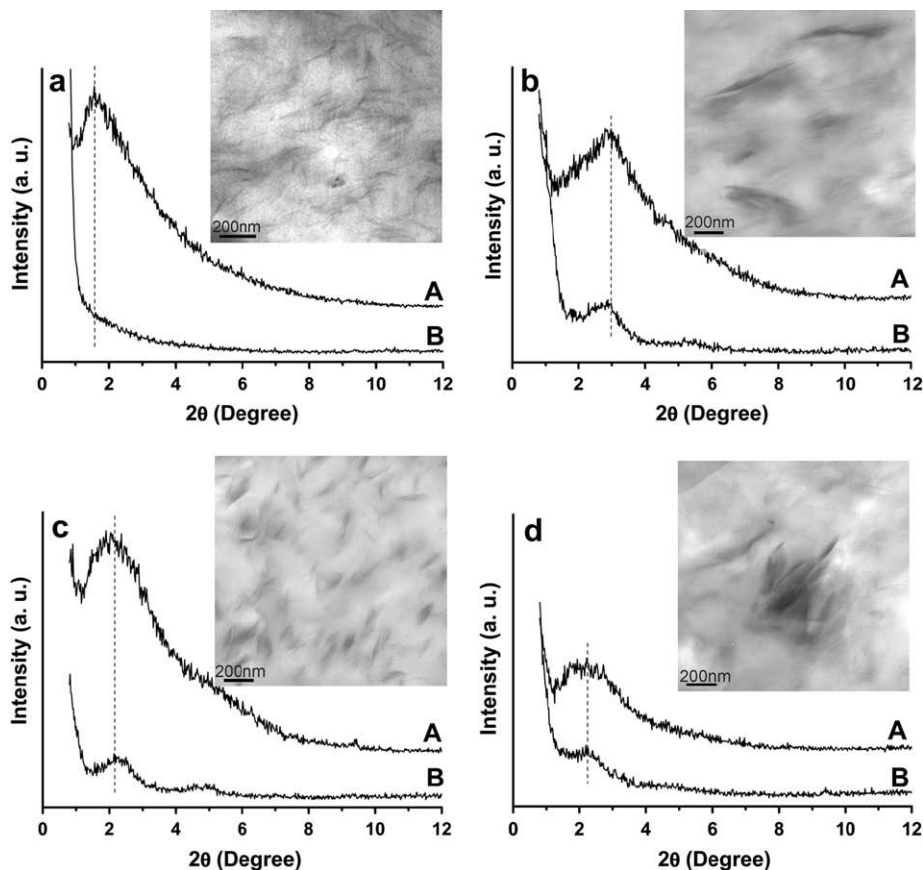**Fig. 8.** Complex viscosities of two kinds of MAPP.

Fig. 9. WAXD profiles and TEM images of the pre-mixtures of MAPP with OMMT-C18 and TPU nanocomposites. (a) A. P-1, B. TPU/P-1; (b) A. P-2, B. TPU/P-2; (c) A. P-3, B. TPU/P-3; (d) A. P-4, B. TPU/P-4.

the MA group of MAPP and the NH group of TPU [20,21]. The formation of hydrogen bonding is evidenced by FTIR spectra (Fig. 10). In Fig. 10a, the absorption peak for NH group in TPU is observed at 3323 cm^{-1} [12]. When TPU is mixed with MAPP, a peak at 3299 cm^{-1} appears, indicating the formation of hydrogen bonding between MAPP and TPU. During the mixing process, some NH groups form hydrogen bonding with MA groups and the corresponding peak shifted to lower wavenumber. Moreover the peak
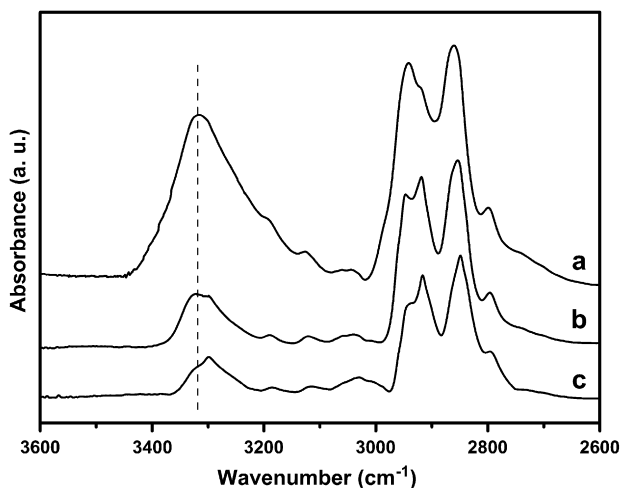

Fig. 10. FTIR spectra of TPU (a), MAPP-1001/TPU = 10/85 (by weight) (b) and MAPP-1010/TPU = 10/85 (by weight) (c).

at 3299 cm^{-1} strengthens as the content of MA group increases, meanwhile the peak at 3323 cm^{-1} weakens (Curve c vs. Curve b in Fig. 10). Thus more hydrogen bonding has been formed between MAPP-1010 and TPU, and accordingly f_2 in the composite containing P-1 is larger than that in the composite containing P-2.

To further testify the roles of f_1 and f_2, OMMT-C18 is pre-mixed with MAPP-1010 in a weight ratio of 1:1 (P-3). Fig. 9c shows that the interlayer distance of OMMT-C18 in P-3 is smaller than that in P-1 due to lesser content of MAPP, and consequently f_1 in P-3 is larger. When P-3 is mixed with the TPU, intercalated structure is obtained, and the size of OMMT-C18 dispersed phase is obviously larger than that in TPU/P-1 system. It proves that the larger interlayer distance weakens f_1, benefiting the exfoliation of OMMT-C18. In addition, OMMT-C18 is pre-mixed with MAPP-1001 in a weight ratio of 1:4 (P-4), and the same interlayer distance as that in P-3 is obtained (Fig. 9d). In this case, f_1 will be the same in both systems [16], thus the effect of f_2 can be verified. When mixing with TPU, the dispersion of OMMT-C18 is very inhomogeneous, and the sizes of OMMT-C18 dispersed phase are large in TPU/P-4 composite. It can be attributed to the weaker f_2 in TPU/P-4 composite due to the less content of MA group in the MAPP-1001. Therefore the dispersion of OMMT-C18 is poor in TPU/P-4 composite. The results suggest that the weaker f_1 and stronger f_2 facilitate to the exfoliation of OMMT-C18.

3.3. The exfoliation process of OMMT-C18 in TPU matrix

To discern the exfoliation process, the intermediate states of TPU/P-1 nanocomposite are characterized (Fig. 11). With the increase of mixing time, the interlayer distance of OMMT-C18
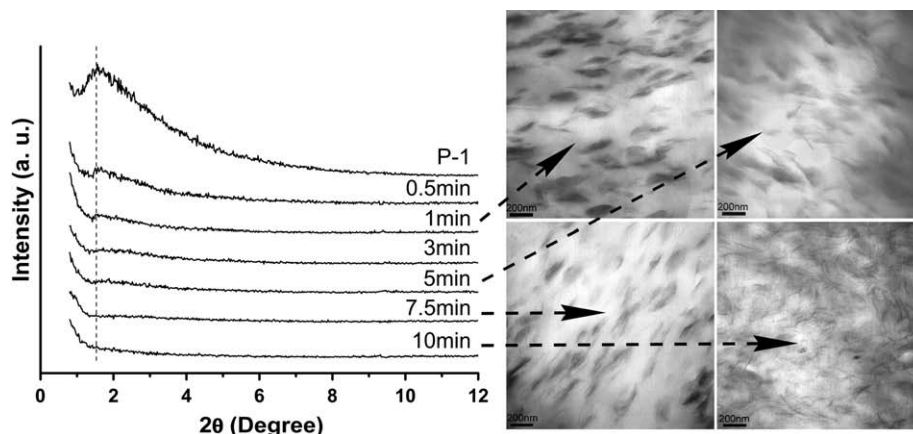
Fig. 11. WAXD profiles and TEM images of TPU/P-1 nanocomposites mixed for different times.

remains unchanged, whereas the intensity of (001) diffraction peak weakens gradually and disappears finally at 10 min of mixing time. It suggests that the further molecular diffusion of TPU is not a main factor for the exfoliation of OMMT-C18. Otherwise the interlayer distance of OMMT-C18 will increase with mixing time. Moreover, the further diffusion of MAPP does not occur during the mixing process, supported by no change of the interlayer distance during prolonging mixing time for preparing P-1. The interlayer distance remains unchanged when the processing time is prolonged from 15 to 25 min, suggesting that no more intercalation occurs after an amount of MAPP-1010 diffuses into the galleries of the organoclay.

According to the comparison of TEM images (Fig. 11), the thickness of dispersed phase reduces gradually under the shear field. Finally, the platelets of OMMT-C18 are exfoliated homogeneously. In TEM images of the samples slightly stained by RuO$_4$ (Fig. 12), some platelets of OMMT-C18 have been exfoliated in TPU matrix when mixed for 5 min (Fig. 12a), and the platelets in P-1 particle enter TPU matrix under shear field (Fig. 12c). When mixed for 10 min, most of OMMT-C18 platelets are exfoliated in TPU matrix, and many platelets still contact with MAPP-1010 phase (Fig. 12b and d). These results confirm that shear stress is a main factor for the formation of exfoliated TPU nanocomposites. Very interestingly, the main role of
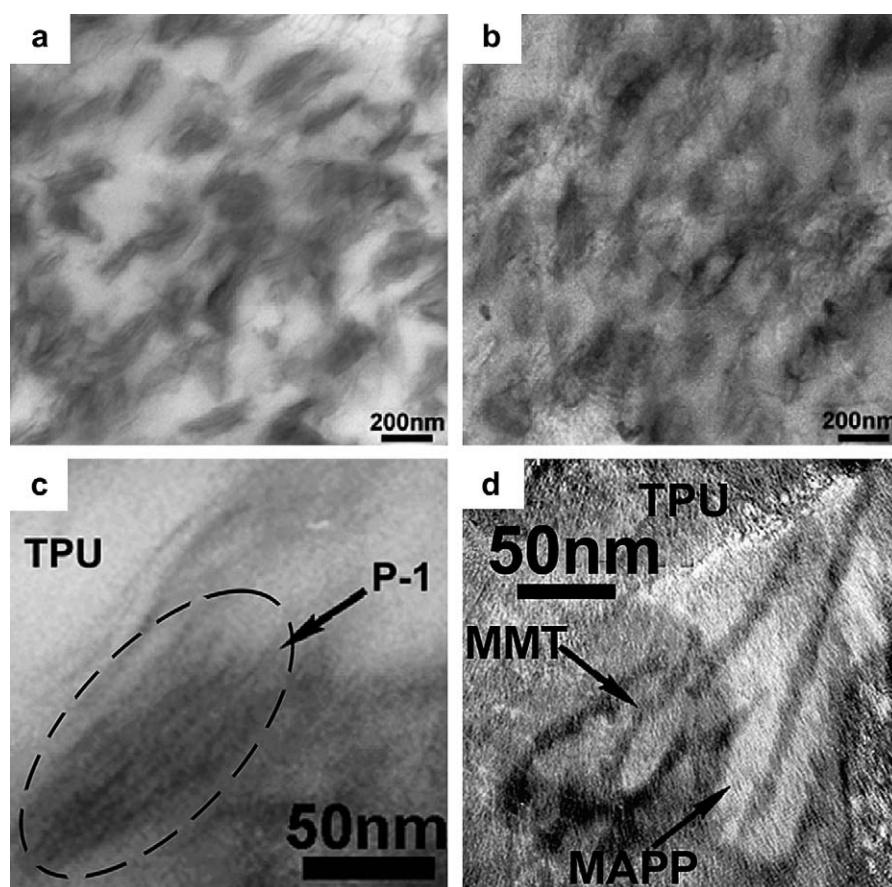

Fig. 12. TEM images of TPU/P-1 nanocomposites mixed for different times stained by RuO$_4$. (a) 5 min; (b) 10 min; (c) high-magnification image of (a); (d) high-magnification image of (b).

Table 1
Mechanical properties and oxygen permeability of TPU nanocomposites.

	Modulus (MPa)	Strength (MPa)	Elongation at break (%)	Oxygen permeability (cm^3(STP)cm/cm^2 s cm Hg)
TPU	43 ± 1.3	34.7 ± 1.4	987 ± 35	2.95 ± 0.02
TPU/MAPP	54.1 ± 3.5	32.9 ± 1.6	872 ± 42	–
Composite-1	73.6 ± 3.1	36.9 ± 1.6	980 ± 40	2.46 ± 0.03
Composite-2	103.4 ± 3.7	35.9 ± 1.3	864 ± 31	2.22 ± 0.03
Composite-3	86.7 ± 3.4	32.1 ± 1.5	781 ± 45	2.37 ± 0.03
Composite-4	72.1 ± 4.1	27.1 ± 1.3	712 ± 43	2.45 ± 0.03
Composite-5	75.1 ± 3.2	27.3 ± 1.4	745 ± 40	–

MAPP in TPU nanocomposites is different from that in PP nanocomposites. In PP nanocomposite, MAPP mainly promotes the compatibility between OMMT and PP [37,38]. However, the compatibility between TPU and OMMT is also good, thus MAPP is not a compatibilizer in TPU nanocomposites. In this case, the intercalation of MAPP weakens the attraction between OMMT platelets, making the platelets exfoliated under shear field.

3.4. The correlation between morphology and properties

The morphology of nanocomposites has a direct effect on the properties, such as mechanical properties and gas permeability. Table 1 shows the mechanical properties and the oxygen permeability of TPU composites. When MAPP-1010 is blended with TPU, the modulus increases, but the strength and the elongation at break decrease slightly, meaning that MAPP-1010 influences the mechanical properties of TPU. The moduli of TPU composites improve remarkably comparing with neat TPU, but the different dispersion states of OMMT-C18 result in the discrepancy of mechanical properties. In Composite-2, the platelets of OMMT-C18 are homogeneously exfoliated, and the effective aspect ratio of OMMT-C18 is larger, which greatly improves the modulus of TPU. As expected, the modulus increment of Composite-2 is the largest among these composites. In Composite-3, the intercalated and exfoliated states coexist; accordingly the modulus increment is obviously smaller than that of Compostie-2. In Composite-4 and Composite-5, the introducing of MAPP-1010 has no contribution to the dispersion of OMMT-C18, thus the moduli of these composites are lower than those of Composite-2 and Composite-3. Moreover, the dispersion of MAPP-1010 in Composite-4 is also inhomogeneous (Fig. 4c), and MAPP-1010 has little contribution to the modulus, thus the modulus of Composite-4 is similar to that of Composite-1.

The tensile strength and the elongation at break of the composites containing MAPP-1010 are smaller than those of Composite-1 because the introducing of MAPP with low molecular weight will decrease the strength and the elongation at break. However, the strength and the elongation of Composite-2 are obviously higher than those of other composites containing MAPP-1010, especially than Composite-3 in which TPU chains experience the same processing time as Composite-2, indicating the good dispersion of OMMT-C18 promotes the strength and the elongation of TPU composites. However, owing to chemical effect of OMMT on the degradation of polymers [33–35], the tensile strength and the elongation at break decrease or only slightly increase compared with neat TPU.

The gas transmission rate of nanocomposites depends on the dispersion state of OMMT-C18 [39,40]. The barrier property of TPU composites becomes better with the increase of the exfoliated level of OMMT-C18 (Table 1). The aspect ratio of dispersion phase augments with the increase of exfoliated level of OMMT-C18, and the path for gas passing is more tortuous when the platelets are exfoliated, thus the oxygen transmission rate will decrease. For example, the platelets of OMMT-C18 are exfoliated in Composite-2, whereas only intercalated state is obtained in Composite-1. Therefore the

oxygen transmission rate of Composite-2 is lower than that of Composite-1. The results suggest that the appropriate introduction of MAPP can optimize the dispersion state of OMMT and thus improve the properties of TPU materials.

4. Conclusion

An effective strategy of exfoliating OMMT by pre-intercalation of a polymer with a lower molecular weight is demonstrated in TPU nanocomposites. The larger interlayer distance of OMMT-C18 achieved by the pre-intercalation of MAPP results in the formation of exfoliated TPU nanocomposites, arising from effectively decreasing the attraction between OMMT-C18 platelets. Consequently the platelets of OMMT-C18 can be easily exfoliated in TPU matrix under shear field. The appropriate molecular structure and melt viscosity of MAPP insure the effective intercalation. The shear force dominates the exfoliation process, and the adequate interaction between MAPP-1010 and TPU is necessary to transfer the shear force in the process of exfoliation. Therefore the larger interlayer distance achieved by the pre-intercalation of the introduced polymer, and the favorable interaction between this polymer and the matrix are the precondition of the strategy for exfoliation. The above results will lay a foundation of further exploration for fabricating the nanocomposites with exfoliated structure.

Appendix. Supplementary data

Supplementary data associated with this article can be found in the on-line version, at doi:10.1016/j.polymer.2009.06.042.

References

[1] Chen-Yang YW, Lee YK, Chen YT, Wu JC. Polymer 2007;48:2969–79.
[2] Rao YQ. Polymer 2007;48:5369–75.
[3] Gintert MJ, Jana SC, Miller SG. Polymer 2007;48:7573–81.
[4] Wang WS, Chen HS, Wu YW, Tsai TY, Chen-Yang YW. Polymer 2008;49:4826–36.
[5] Zhu JJ, Wang XL, Tao FF, Xue G, Chen TH, Sun PC, et al. Polymer 2007;48:7590–7.
[6] Kojima Y, Usuki A, Kawasumi M, Okada A, Fukushima Y, Kurauchi T, et al. J Mater Res 1993;8:1185–9.
[7] Alexandre M, Dubois P. Mater Sci Eng R 2000;28:1–63.
[8] Ray SS, Okamoto M. Prog Polym Sci 2003;28:1539–641.
[9] Balazs AC, Singh C, Zhulina E. Macromolecules 1998;31:8370–81.
[10] Meng XY, Wang Z, Zhao ZF, Du XH, Bi WG, Tang T. Polymer 2007;48:2508–19.
[11] Lyatskaya Y, Balazs AC. Macromolecules 1998;31:6676–80.
[12] Dan CH, Lee MH, Kim YD, Min BH, Kim JH. Polymer 2006;47:6718–30.
[13] Chavarria F, Paul DR. Polymer 2006;47:7760–73.
[14] Finnigan B, Martin D, Halley P, Truss R, Campbell K. Polymer 2004;45:2249–60.
[15] Fermeglia M, Ferrone M, Pricl S. Fluid Phase Equilib 2003;212:315–29.
[16] Bousmina M. Macromolecules 2006;39:4259–63.
[17] Heinz H, Vaia RA, Farmer BL. J Chem Phys 2006;124:224713–21.
[18] Zhao ZF, Tang T, Qin YX, Huang BT. Langmuir 2003;19:9260–5.
[19] Fornes TD, Hunter DL, Paul DR. Macromolecules 2004;37:1793–8.
[20] Tang T, Jing XB, Huang B. J Macromol Sci Phys 1994;B33:287–305.
[21] Lu QW, Hoye TR, Macosko CW. J Polym Sci Part A Polym Chem 2002;40:2310–28.
[22] Vo LT, Giannelis EP. Macromolecules 2007;40:8271–6.
[23] Khatua BB, Lee DJ, Kim HY, Kim JK. Macromolecules 2004;37:2454–9.
[24] Lu QW, Macosko CW. Polymer 2004;45:1981–91.
[25] Yang J, Chen X, Fu R, Zhang M, Chen H, Wang J. J Appl Polym Sci 2008; 109:3452–7.
[26] Chun BC, Cho TK, Chong MH, Chung YC, Chen J, Martin D, et al. J Appl Polym Sci 2007;106:712–21.
[27] Zhao ZF, Tang T, Qin YX, Huang BT. Langmuir 2003;19:7157–9.
[28] Szazdi L, Pukanszky JB, Foldes E, Pukanszky B. Polymer 2005;46:8001–10.
[29] Shen Z, Cheng YB, Simon GP. Macromolecules 2005;38:1744–51.
[30] Fornes TD, Yoon PJ, Keskkula H, Paul DR. Polymer 2001;42:9929–40.
[31] Chen GM, Liu SH, Chen SJ, Qi ZN. Macromol Chem Phys 2001;202:1189–93.

[32] Chaiko DJ, Leyva AA. Chem Mater 2005;17:13–9.
[33] Zanetti M, Kashiwagi T, Falqui L, Camino G. Chem Mater 2002;14:881–7.
[34] Qin HL, Zhang SM, Zhao CG, Hu GJ, Yang MS. Polymer 2005;46:8386–95.
[35] Song L, Hu Y, Tang Y, Zhang R, Chen Z, Fan W. Polym Degrad Stab 2005;87:111–6.
[36] Wang PS, Chiu WY, Chen LW, Denq BL, Don TM, Chiu YS. Polym Degrad Stab 1999;66:307–15.
[37] Kawasumi M, Hasegawa N, Kato M, Usuki A, Okada A. Macromolecules 1997;30:6333–8.
[38] Reichert P, Nitz H, Klinke S, Brandsch R, Thomann R, Mulhaupt R. Macromol Mater Eng 2000;275:8–17.
[39] Gusev AA, Lusti HR. Adv Mater 2001;13:1641–3.
[40] Osman MA, Mittal V, Lusti HR. Macromol Rapid Commun 2004;25:1145–9.